12th International Conference on CANDU Fuel
Holiday-Inn Waterfront Hotel
Kingston, Ontario, Canada, 2013 September 15-18

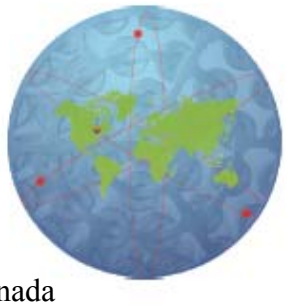

EXAMINING THE VIABILITY OF ULTRASONIC INSPECTION OF DISCHARGED CANDU®[i] FUEL BUNDLES

T.W. Krause[1], W.H. Huang [2], and B.J. Lewis[3]
[1]Department of Physics, Royal Military College of Canada, Kingston, Ontario, Canada
(P.O. Box 17000, Station Forces, K7K 7B4, 613 541 6000 x6415, Thomas.Krause@rmc.ca)
[2]Department of Chemistry and Chemical Engineering, Royal Military College of Canada
[3]Faculty of Energy Systems and Nuclear Science, University of Ontario Institute of Technology

ABSTRACT –Ultrasonic testing (UT) methods may provide a more sensitive means of inspecting compromised fuel elements within fuel bundles discharged from CANDU® reactors, when compared with visual inspection techniques that are presently used. This is accomplished through identification of water ingress. This work presents a demonstration of UT capability to differentiate between conditions of water ingress and absence of water in fuel elements containing un-irradiated uranium dioxide pellets. Results obtained from tests of angled beam UT established that water in a defective fuel element acts as a couplant for sound waves, generating acoustic signatures from between fuel pellets within the element.

Introduction

The CANDU® (CANadian Deuterium Uranium) reactor uses bundles of uranium fuel elements as its fuel source. The uranium fuel elements consist of ~30 pellets stacked within a sealed Zircaloy-4 sheath, with welded end caps. 37 fuel elements are arranged in a pattern of concentric circles welded to end plates, resulting in a bundle of 0.5 m length. Typically, less than 0.1% [1] of the fuel elements are detected as defective by visual inspection methods [2]. In general there are four major causes of fuel defects, including debris fretting, stress corrosion cracking, delayed hydrogen cracking and manufacturing flaws [3]. Among these, fretting is currently the most probable cause of fuel failure. Fuel elements located around the outer most ring of the bundle in general deteriorate faster because of their higher fuel ratings.

In the event of a compromised fuel sheath, circulating coolant can enter into the element, coming into direct contact with fuel pellets. Since the temperature in the gap between fuel pellet and sheath is higher than the saturation temperature, the liquid coolant flashes to steam that can diffuse along the entire fuel-element length. The consequent effect is a reduction in thermal performance of the fuel element, with a possibility for fuel centerline melting at high power operation or during reactor upset conditions. Since the presence of molten fuel can result in the breach of a fuel sheath, the prevention of significant fuel oxidation is important [4,5]. Furthermore, fission products may also be released into the primary coolant when the fuel element fails, increasing radiation exposures for station personnel. It is therefore useful for the station to discharge the defective fuel bundle as soon as operationally possible. Currently, there is no efficient method of confirming that a defective bundle has been discharged other than by observing a decrease in coolant activity levels.

[i] CANDU is a registered trademark of Atomic Energy of Canada Limited (AECL).

A post-irradiation examination (PIE) of any defective bundle is of benefit to the utility to better understand the root cause of failure. An effective PIE technique for use in the fuel bays, such as ultrasonic testing (UT), could be immediately applied after discharge of a suspect fuel bundle, to confirm and characterize a defective fuel bundle. The UT system could be adapted to tools such as FEMER (Fuel Envelope MEasuring Rig), which can precisely position bundles and which has been designed to facilitate in-bay bundle profiling [2]. Ultrasonic testing (UT) is already extensively used in the nuclear industry for periodic inspection of in-reactor pressure tubes [6,7] and by the LWR industry to detect the presence of water in the plenum of fuel rods, which is an indication of fuel failure [8]. UT probes have a demonstrated capability of performance under these high radiation flux conditions within the pressure tubes [6,7].

This paper examines the viability of using UT for the inspection of fuel elements, which may potentially have been compromised, expanding on previous work [3] by consideration of higher frequencies and the source of physical generation of acoustic modes from between fuel pellets within the fuel element. Water ingress is observed to provide the opportunity to profile fuel pellet geometry within the fuel element. As well, a platform for UT could accommodate profiling of fuel bundle deformation, detection of cracking in end plates and fuel element sheath profiling.

1. Previous studies

During inspection of un-irradiated fuel bundles, UT or Eddy current testing (ECT) are employed for quality-assessment (QA) purposes [9]. Post-reactor operation inspection is performed on fuel bundles when fuel elements are suspected of containing a sheath defect [2,10,11]. Developments in the post-operation inspection have mostly targeted PWR and BWR reactors [12,13]. The use of ultrasound to distinguish between fuel rods that are either full or free of water has been proposed previously for light water reactors (LWR) [12]. LWR rods are assembled as a square array structure. The inspection is done in a fuel bay, where fuel is temporarily stored after it has been removed from the core. The post-operation inspection method involves movement of a single ultrasonic transducer parallel to the length of a fuel element within the assembly. The idea of generating circumferential Lamb waves to detect the presence of water within PWR fuel rods using resonance backscattering theory from ultrasonic pulses has also been demonstrated [13]. In this case ultrasonic pulses were introduced perpendicular to the surface of the fuel-element cladding. The Lamb waves were detected based on whether or not the received signal exhibited a series of periodic echoes. In the presence of such signals, it was inferred that the fuel rod did not contain water. However, if no periodic signal was received, then the rod was believed to contain water. In the latter case of a defective fuel rod, a perturbation of the scattered waves was produced due to water assisted reflection at the fuel pellet surface [13].

The method proposed in this work is specifically aimed at ultrasonic based inspection of CANDU fuel elements. The shape and configuration of the fuel bundles, orientated horizontally within the pressure tube, are cylindrical and not in a square array assembly as for the PWR fuel design. So far a UT inspection technique has not been developed for CANDU applications; hence, this research is intended to address this need. In general, only visual inspection is performed in the fuel bays to identify suspect bundles, which then undergo a more detailed metallographic examination for determination of root cause of failure.

2. Theory

Propagation of the ultrasonic beam from the liquid environment through the surface of the fuel element sheath, results in interaction of the acoustic wave with first, the Zircaloy-4 fuel sheath and second, for an intact fuel element, helium fill gas. In the case of a defective rod water may be present and the ultrasound will be more strongly coupled to components within the fuel element such as the fuel pellets themselves. At each individual interface, the intensity of the sound transmitted through, as well as reflected from, the interface between two media is a function of the respective acoustic impedance and the angle of incidence. Acoustic impedance "Z" has units of grams per square centimetre-second and is given by: [14].

$$Z = \rho V \tag{1}$$

where ρ is the density of the medium and V is the velocity. There are three modes of acoustic wave transmission considered here for inspection of fuel elements. The modes are the (i) longitudinal, (ii) shear, and (iii) Lamb wave modes. For inspection of thicker fuel bundle components, such as the end plate, longitudinal and shear wave modes are of interest. For application of conventional UT, probe excitation frequencies range between 2.25 and 10 MHz. For high frequency surface profiling higher frequencies are of interest, for example that provided by a 20 MHz focused beam transducer.

The acoustic interaction relevant to fuel bundle inspection in a fuel bay environment is the water-to-solid interface. Figure 1 indicates the ultrasonic ray geometries for interaction of acoustic waves at an interface between Medium 1 (water) and Medium 2 (solid). The incident beam has longitudinal velocity V_{L1}, at angle θ_{L1} with respect to the interface normal, and reflected velocity $V_{L1'}$, at angle θ_{L1} in Medium 1. In Medium 2 (Zircaloy-4 in the case of a fuel element sheath) a transmitted longitudinal V_{L2}, and shear wave component V_{S2}, as indicated in Figure 1, are present. The second interface of the fuel element sheath is not depicted, but would be expected to generate additional modes such as standing waves, within the fuel element [15,16].

As indicated in Figure 1, after the acoustic wave propagates out of the probe, the first interface that the beam encounters is the water-Zircaloy boundary, which is the interface of interest since various wave modes will be produced within this volume. The presence of longitudinal, shear and finally Lamb wave modes in the fuel sheath is a function of the critical angles obtained from Snell's law under oblique incidence given in [14,15,17] as

$$\frac{\sin\theta_{L1}}{V_{L1}} = \frac{\sin\theta_{L2}}{V_{L2}} = \frac{\sin\theta_{S2}}{V_{S2}}. \tag{2}$$

Relevant ultrasonic properties for water and Zircaloy are summarized in Table 1. The first critical angle is calculated by setting θ_{L2} equal to 90° and using the values in Table 1 for V_{L1} (speed of longitudinal wave in water) and V_{L2} (speed of longitudinal wave in Zircaloy metal)

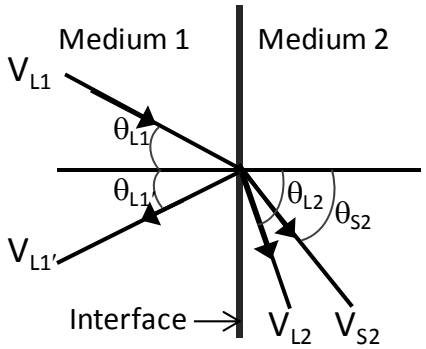

Figure 1: Definitions Ray Parameters (Incident angle θ_{L1} with respect to interface normal, at velocity V_{L1} in Medium 1 (water) and reflected ray with $V_{L1'}$, and in Medium 2 (Zircaloy) transmitted longitudinal and shear wave rays, with velocities V_{L2} and V_{S2}, respectively).

Equation 2 yields $\theta_{Lc1} \approx 18°$. Beyond θ_{Lc1} no longitudinal wave component exists in the material. Similarly, with $V_{L1} = 1.48$ km/s (speed of longitudinal wave in water) and V_{S2} (speed of shear wave in Zircaloy metal) the second critical angle is calculated to be $\theta_{Lc2} \approx 39°$.

Table 1: Ultrasonic Properties for Water and Zircaloy

Material	Frequency (MHz)	ρ (g/cm^3)	V_L (km/s)	Wavelength λ_L (mm)	V_S (km/s)	Wavelength λ_S (mm)
Water	2.25	1.0	1.48	0.66	N/A	N/A
	5	1.0	1.48	0.3	N/A	N/A
Zircaloy	2.25	6.57 [18]	4.72	2.10	2.36	1.05
	5	6.57 [18]	4.72	0.94	2.36	0.47

For a beam with oblique incidence ($\theta_{L1} \neq 0$), the shear wave transmission coefficient T_S for longitudinal waves is expressed as [19]:

$$T_S = \left(\frac{\rho_1}{\rho_2}\right) \frac{2Z_{S2}cos2_{S2}cos\theta_{L2}cos\theta_{L1}}{\left(Z_{L2}cos^2 2_{S2}cos\theta_{L1}\cos\theta_{S2} + Z_{S2}sin^2 2_{S2}cos\theta_{L1}cos\theta_{L2} + Z_{L1}cos\theta_{L2}\cos\theta_{S2}\right)} \quad (3)$$

where angles are defined in Figure 1 above. A similar expression has been obtained for the longitudinal wave transmitted energy component with angle ray angle θ_{L2}. Substitution of Equation 2 into 3 can be used to show that beyond the second critical angle, no shear wave energy is transmitted into the material. Instead, different modes of wave propagation may be introduced including surface waves and Lamb waves [14]. Lamb waves can propagate in plates up to a few wavelengths thick. This is possible in the 0.4 mm thick fuel element sheath, given the wavelengths of 2.1 mm and 0.9 mm, as indicated in Table 1 for the 2.25 MHz and 5 MHz central frequencies, respectively. Lamb waves are complex vibrations governed by the boundary conditions of the medium. Two forms of Lamb waves exist: (i) symmetrical and (ii) asymmetrical [14,15,16]. Figure 2 shows a depiction of the first modes of the symmetrical (L_{11}) and asymmetrical (L_{21}) Lamb waves [14]. The motions of the medium's particles, whether

symmetrical or asymmetrical relative to the axis of the material, determine the wave form. Symmetrical waves consist of longitudinal particle displacements and asymmetrical waves of shear displacements. The velocity of the waves varies with the angle with which the wave enters the medium. Therefore, wave velocities are the result of a combination of plate boundary conditions, wave frequency, and angle of incidence [14]. The frequency x plate thickness factor of 0.9 at 2.25 (MHz mm) and of 2.0 at 5.0 MHz suggests that only lower modes beginning with L_{11} and L_{21} will be excited for the experimental configurations considered here. However the number of modes increases with the product of frequency and plate thickness [14].

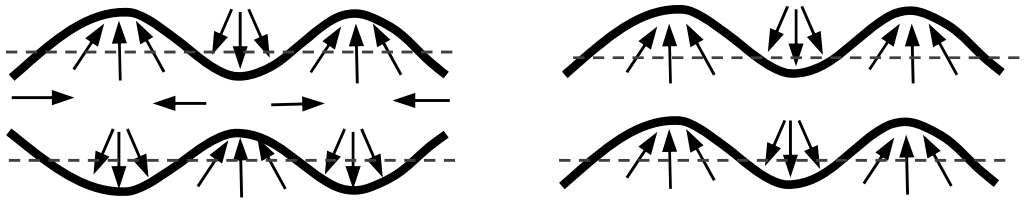

(a) (b)

Figure 2: First Modes Depicted for a) Symmetrical (L_{11}) and b) Asymmetrical (L_{21}) Lamb Waves (arrows indicate particle motion vectors for horizontal axis wave propagation [14]).

During an inspection, the ultrasonic wave, from the surrounding water, medium 1, will impact the fuel element sheath in the absence of exterior fixtures such as bearing pads and end caps. For the case of water ingress into a defective fuel element, additional reflections from within the element, including from the fuel pellets may arise. Under conditions of an intact fuel element, helium fill gas within the sheath will result in little or no energy transmission. The acoustic impedance for normal incidence from the fuel sheath in this case is very high ($4.42 \cdot 10^6 g/(cm^2 \cdot s)$ from Table 1 and Equation (1)). Percentage of intensity being transmitted into the helium fill gas from the sheath is negligible and is calculated for a longitudinal wave to be $T_{Sheath\text{-}He\ gas} \approx 0.0016$ % [3]. It is expected that ultrasonic scanning of an uncompromised fuel element will only exhibit signals from the back-wall reflections of the fuel sheath. Under conditions where water is present in the fuel element, a transmission factor is calculated as $T_{sheath\text{-}water} = 12.5\%$. With water present in a defective element there will be a change in intensity in the received signal due to reflections back from internal structures, such as the fuel pellets, within the element. Signals will continue to be modified as as the incident wave angle varies past the first and second critical angles.

3. Experimental Setup

During the preparation stage, one of two fuel elements containing actual unirradiated UO_2 pellets was modified on the end caps to permit replacement of He fill gas in the 50 μm radial gap between the sheath and fuel pellets with water, thereby simulating water ingress within a defective fuel element. A second fuel element was not modified as a control and for comparison purposes. The elements were on the order of 13.0 mm in diameter and 494.5 mm in length. The Zircaloy sheath was measured to be 0.4 mm thick, which is within tolerance for manufactured fuel sheath thickness of 0.41±0.025 mm.

Figure 3: Inspection Set-up with Ultrasonic Probe Adjusted for Oblique Incidence

The ultrasonic inspection system (TecScan of Boucherville, Quebec), was composed of three components: (i) X-Y axis actuators, (ii) a system amplifier, and (iii) a processor/display. Figure 3 shows the inspection set-up with the probe adjusted for oblique incidence. During operation, two axis controllers moved the probe, allowing it to traverse and inspect the surface of the specimen. The UT inspection software (TecView), installed on a PC with a Windows operating system, controlled the motion of the two axis actuator system and recorded the calibrated position of the probe. Data was acquired as a single line scan along the fuel element. Measurements were performed at Stern Laboratories, Hamilton.

4. Results

An analysis of measurements obtained at 2.25 and 5 MHz under various conditions of normal and oblique incidence was conducted. Data was presented as a series of B-Scans, which depict ultrasonic amplitude in grey scale as function of position on the horizontal axis and on the vertical axis as a function of time. Figure 4 and Figure 5 show ultrasonic scans for intact and defective fuel elements obtained at 2.25 MHz for normal incidence, without and with internal water present, respectively. In Figure 4 only interface reflections, bearing pads and fuel element ends (bright lines near the left and right edges of the figure) are visible when internal water is absent. When water is present in a defective fuel element, clear demarcation of the fuel pellets and measurement of their length is possible as shown in Figure 5. Resolution of the fuel pellets, showing up as brighter 16 mm long reflections with darker gaps is facilitated by the presence of water as a couplant, as described by normal incidence transmission through the sheath with subsequent return reflections [19]. The 16 mm length is the fabricated length of the pellets [1].

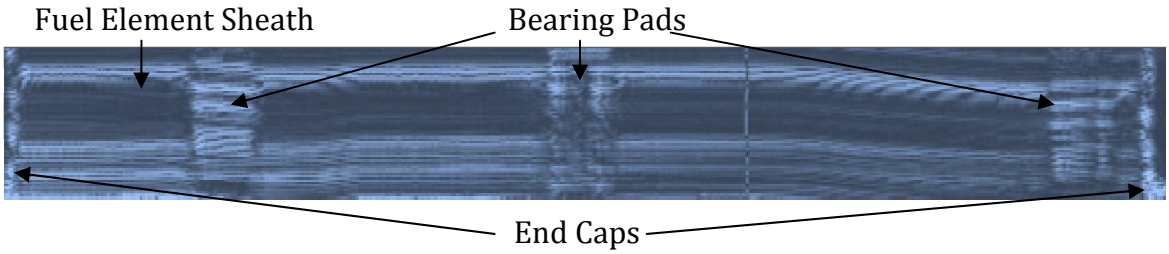

Figure 4: B-Scan of Intact Fuel Element at Normal Incidence - Horizontal Axis is Position - Vertical Axis Time

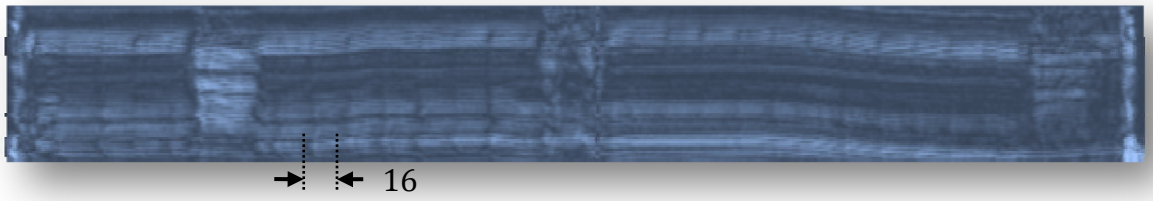

Figure 5: B-Scan of a Defective Fuel Element at Normal Incidence with Visible Fuel Pellets

The most representative oblique incident angles are 30°, 40° and 50°, which correspond to shear wave mode (after 1st critical angle), second critical angle, and Lamb wave mode (beyond 2nd critical angle), respectively. Figure 6, taken at 30° incidence, after the first critical angle (shear mode only), illustrates the ultrasonic B-scan of an intact fuel element. As in the case of normal incidence only the sheath interface signal, bearing bad edges and end caps are evident. Figure 7 illustrates the ultrasonic B-scan of a defective fuel element at 30° incidence with a blow up of part of the scan to show more details. Inspection of the defective fuel element using a probe at a 30° incident angle reveals significant water ingress characteristics, with little back-wall signal distortion that was present in the normal oriented scans (Figure 5). Distinctive slanted periodic stripes, which were not observed in intact fuel elements as shown in Figure 6, are now present. These stripes are approximately 16 mm apart, corresponding to the length of individual fuel pellets [1]. Figure 8 illustrates the ultrasonic B-scan of a defective fuel element with ultrasound at 40° incidence and a blow up of part of the scan to show more details. Acoustic signals show up as stronger periodic slanted stripes, corresponding to fuel pellet ends with only a weak sheath interface signal, when compared with 30° incidence. At 40° incidence just beyond the second critical angle (39° from Eqn. (2) and Table 1) for shear waves, acoustic energy from the generation of Lamb waves is beginning to emerge. Figure 9 shows the B-Scan response for a defective fuel element with 50° beam incidence at 2.25 MHz (a) and 5 MHz (b), respectively. The Zircaloy sheath interface signal is now completely absent in the B-scan. Only the periodic stripes, which provide a clear demarcation of fuel pellet ends, are observed. The 2.25 MHz scan in (a) provides more acoustic signal than both the 5 MHz signal in (b) and the signal obtained at 40° incidence as shown in Figure 8. This is attributed to a larger amount of acoustic energy being transmitted to the fuel element interior, through the Lamb wave mode, with correspondingly stronger reflections between fuel pellet ends.

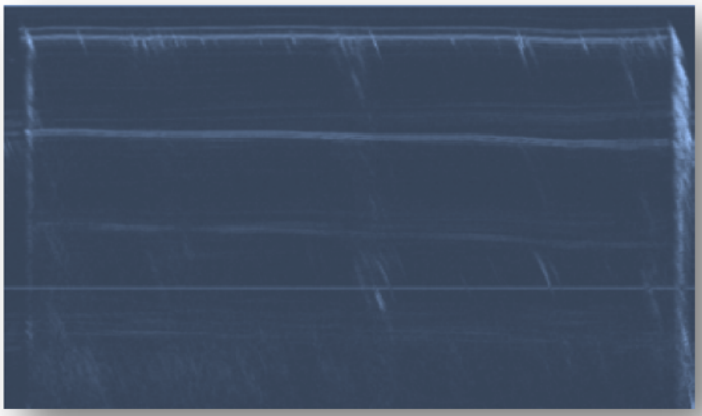

Figure 6: **2.25 MHz B-Scan of an Intact Fuel Element with 30° Incident Beam**

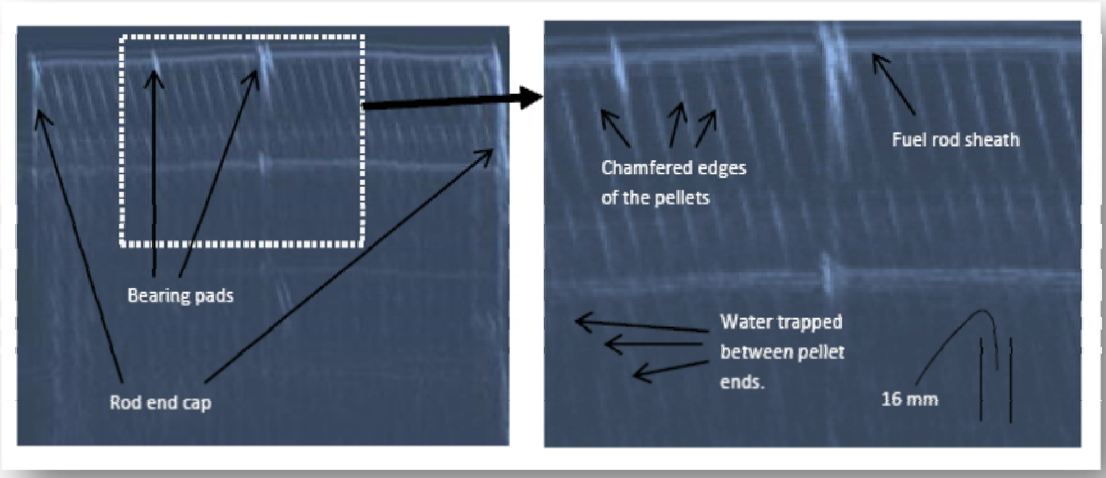

Figure 7: **2.25 MHz B-Scan of Defective Fuel Element with 30° Incident Beam**

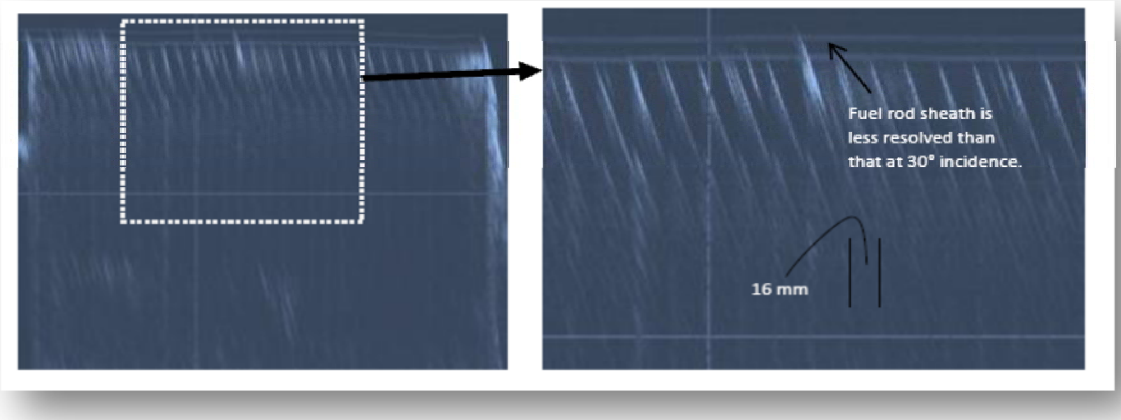

Figure 8: 2.25 MHz B-Scan of Defective Fuel Element with 40° Incident Beam

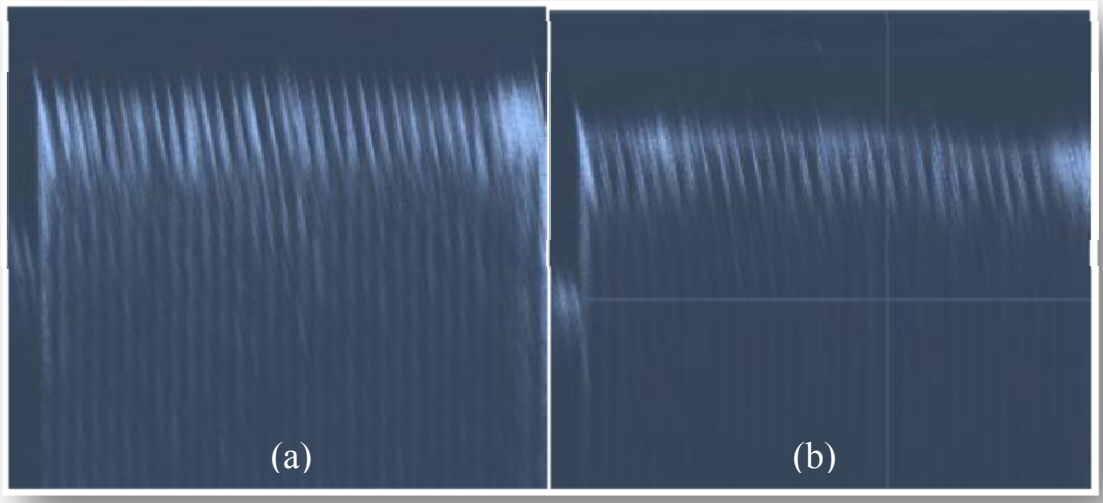

Figure 9: B-Scan for a) 2.25 MHz and b) 5 MHz Transducer at 50° Incident Angle

5. Discusion

Normal incidence, as shown in Figure 5 demarcates fuel pellet ends and therefore, could be used to provide information on internal fuel pellet structures in fuel elements discharged from reactors in the presence of a defect that has allowed water ingress. As shown in Figure 7 through Figure 9, the rectangular cross section of the sheathing gradually disappears as the incident angle increases. At angles greater than the first critical angle, the transmitted shear waves provide clearer demarcation of fuel pellets than the normal incident mode. However, after the second critical angle (~39°), the interface signal disappears and the Lamb wave mode becomes the dominant acoustic mode in the Zircaloy sheath. The Lamb waves induce longitudinal waves in the water within the element and these strongly interact with fuel pellet ends. The long slanted stripes in the B-Scans in this case are attributed to acoustic reflections arising in the trapped water between the pellet ends. These trapped internal reflections act as an increasingly delayed source of sound, which is still sensed as the transducer continues its motion along the fuel element. It appears that at 50° for the 2.25 MHz transducer, greater energy transfer to the interior arises, as the stripes are most noticeable. This suggests that the angle range (50°-55°) would be the optimum scan angle for the Lamb wave mode at 2.25 MHz, as suggested previously [3]. 30° incidence would be optimum if only a shear wave mode was used [3].

The difference between the 2.25 MHz and 5 MHz frequencies in Figure 9 is attributed to the number of Lamb wave modes that may be generated in the sheath. At 2.25 MHz the frequency x thickness factor is 0.9 MHz mm compared with 2.0 MHz mm for the 5.0 MHz transducer. It is possible that higher modes are excited in the Zircaloy material at 5.0 MHz [16], which in turn reduces the energy transmitted through the sheath and therefore, the acoustic energy that is coupled to the spaces between the pellets.

This paper has examined the viability of using UT for the inspection of fuel elements, which are defective to the extent that water can penetrate the interior of the element. The work has demonstrated the ability to observe fuel pellets within the element when internal water is present. Development of an ultrasonic inspection system for irradiated elements could also provide a platform for the development of high frequency ultrasonic focused beam profiling of irradiated fuel sheaths. Profiling of irradiated sheaths could provide key information for the inference of fuel bundle condition under reactor operating conditions. High resolution profiling could also contribute to assessment of lower frequency ultrasonic inspection for water ingress, since variations in the fuel sheath profile are anticipated to affect the low frequency ultrasound reflections.

6. Conclusions

This work examined the use of ultrasonic techniques for the potential inspection of post-irradiated fuel bundles discharged into fuel bays, as a means of identifying failed fuel elements when water ingress is present. Ultrasound was used to identify the occurrence of a defective element by exploiting coupling of acoustic sound between fuel pellets in such defective elements. This work evaluated different angles of ultrasound incidence, as well as transducers operated at frequencies of 2.25 and 5.0 MHz. Results were examined for generation of ultrasound at normal and oblique incidence, generating longitudinal, shear and Lamb wave modes, with consideration of the various critical angles under which these modes occur. Under oblique incidence the coupled acoustic signature appeared as periodic “stripes” in a B-Scan display, which was attributed to acoustic reflections in the water between fuel pellet ends. Oblique incidence provided improved results in this study, suggesting that this method be the focus of future investigations on actual irradiated fuel elements.

7. References

[1] B.J. Lewis, R. D. MacDonald, N.V. Ivanoff and F.C. Iglesias, "Fuel Performance and Fission Product Release Studies for Defected Fuel Elements," *Nuclear Technology*, Vol. 103, 1993, p 220-245.

[2] J. St-Pierre, “Fuel Performance Evaluation Bruce Power & OPG CANDU Stations.” 3rd International CANDU In-Service Inspection and NDT in Canada 2010 Conference, Hilton Suites, 8500 Warden Avenue, Markham, Ontario, 2010 June 14-17, 2010.

[3] W.H. Huang, T.W. Krause and B.J. Lewis, “Laboratory Tests of an Ultrasonic Inspection Technique to Identify Defective CANDU Fuel Elements.” *Nuclear Technology*, Vol. 176, December, 2011, 452-461.

[4] A. Viktorov, and M. Couture, “Regulatory Activities in the Area of Fuel Safety and Performance.” Canadian Nuclear Safety Commission, Presented at the 9th International Conference on CANDU Fuel, Belleville, September 17-21, 2005.

[5] M. J. Welland, B. J. Lewis and W. T. Thompson, "Review of high temperature thermochemical properties and application in phase-field modelling of incipient melting in defective fuel," Journal of Nuclear Materials, 412 (2011) 342-349.

[6] D. Heinrich, G. Müllera and M. Weissa, "Mechanized in-service ultrasonic inspection of austenitic welds in nuclear plants", *Ultrasonics*, Vol. 15, 1982, p 152.

[7] M. Trelinski, "Application of Ultrasonic Testing Methods for Volumetric and Surface Inspection of CANDU Pressure Tubes", NDT, Vol.4, Iss. 2, 1999.

[8] IAEA, "Review Of Fuel Failures In Water Cooled Reactors", IAEA Nuclear Energy Series No. NF-T-2.1, 2010.

[9] W.R. Dams, R. Baumann, I. Hanel, B. Happ and L. Heins, "Fabrication of UO2 fuels with non-destructive assay and rod scanner technology for production and final quality control", Journal of Nuclear Materials, Vol. 178, Iss. 2-3, 1991, 171-178.

[10] J.N. Lillington, "The Future of Nuclear Power" Elsevier Ltd, (2004).

[11] W.T. Nuttall, and K. Hancox, "The Canadian approach to safe, permanent disposal of nuclear fuel waste", *Nuclear Engineering and Design*, Vol. 129, Iss. 1, 1991, p 109-117.

[12] B.L.F. van Swam, R. Thomas, H. D. Quang, "Method and apparatus for detecting failed fuel rods", accessed 09, Sept., 2008, <http://www.patentstorm.us/patents/4879088/fulltext.html>.

[13] M.S. Choia, Y. Kim, and H.C. Kim, "Detection of leak-defective fuel rods using the circumferential Lamb waves excited by the resonance backscattering of ultrasonic pulses", *Ultrasonics*, Vol. 30, Iss. 4, 1992, p 221-223.

[14] D. E. Bray, R. K. Stanley, "Nondestructive Evaluation", McGraw-Hall, Inc. (1989), p 80.

[15] Y. B. Cohen, A.K. Mal, ASM Committee, "Nondestructive Evaluation and Quality Control", 9th Edition, American Soc. for Metals International, Ohio (1989).

[16] C. Hellier, "Handbook of Nondestructive Evaluation", 1st Edition, McGraw-Hill Professional, (2001).

[17] W. L. Schmerr, "Fundamentals of Ultrasonic Nondestructive Evaluation: A Modeling Approach", 1st Edition, Springer Publishing, Co. (1998).

[18] L.S. Rubenstein, "Properties of Zircaloy-2," *Nucleonics*, **17**, (1959) 72.

[19] J. David and N. Cheeke, "Fundamentals and Applications of Ultrasonic Waves", 2nd Edition, CRC Press, NY (2012).